

Topological superconductivity in Dirac semimetals

Shingo Kobayashi and Masatoshi Sato

Department of Applied Physics, Nagoya University, Nagoya 464-8603, Japan

(Dated: March 1, 2022)

Dirac semimetals host bulk band-touching Dirac points and a surface Fermi loop. We develop a theory of superconducting Dirac semimetals. Establishing a relation between the Dirac points and the surface Fermi loop, we clarify how the nontrivial topology of Dirac semimetals affects their superconducting state. We note that the unique orbital texture of Dirac points and a structural phase transition of the crystal favor symmetry-protected topological superconductivity with a quartet of surface Majorana fermions. We suggest possible application of our theory to recently discovered superconducting states in Cd_3As_2 .

Dirac semimetals are three-dimensional (3D) materials that possess gapless (Dirac) points in the bulk Brillouin zone (BZ), whose low-energy excitations are effectively described as Dirac fermions. With time-reversal symmetry (TRS) and inversion symmetry (IS) preserved, a pair of Dirac points is formed at the crossing of two doubly degenerate bands on a high-symmetry axis. They are protected by discrete rotation (C_n) symmetry [1–4], which prohibits band mixing to open a gap. Furthermore, Dirac semimetals may host a surface Fermi loop (FL) [3–6]. This contrasts sharply with a surface Fermi arc in Weyl semimetals [7] because its topological origin is different. Several Dirac semimetals, including Na_3Bi [8–11] and Cd_3As_2 [5, 6, 12–17], have been demonstrated experimentally and predicted theoretically [18–22].

Superconducting phase transitions were reported recently in Cd_3As_2 [23–25] and Au_2Pb [26], both of which support Dirac points protected by C_4 symmetry. Bulk Cd_3As_2 exhibits superconductivity under high pressure (~ 8.5 GPa) [25] accompanied by a structural phase transition of the crystal [27]. In addition, point contact measurements of Cd_3As_2 reportedly induce superconductivity around the point contact region, where the tunneling conductance shows a zero-bias conductance peak [23, 24]. Au_2Pb also exhibits a superconducting phase transition after a structural phase transition [26].

In this letter we address the effect of the nontrivial topology, i.e., the Dirac points and FL, on the superconducting properties. Topological materials are a promising platform to realize topological superconductors (TSCs) owing to the nontrivial topology of the wave function in normal states [28–33]. For instance, surface Dirac fermions may realize a TSC even for an s -wave pairing state [28, 29]. Also, the Fermi surface topology, which is the simplest topological structure in the normal state, directly affects the topological superconductivity of odd-parity superconductors [30, 34]. For the carrier-doped topological insulator, topological superconductivity has been anticipated for the surface [29] or the bulk [30].

Here we present a general framework for studying superconductivity in Dirac semimetals. The key ingredients are symmetry-protected topological numbers in crystalline insulators and superconductors [35–46]. In

particular, we examine the C_4 topological invariant and the mirror Chern number, which ensure the existence of Dirac points and FLs, respectively, in Dirac semimetals. First, we show that these two topological numbers are intrinsically related to each other, establishing a relation between Dirac points and surface FLs. Then, we elucidate how the nontrivial topology of Dirac semimetals affects their superconducting state. We find that for a class of pairing symmetries, Dirac points and FLs in the normal state are inherited as bulk point nodes and surface Majorana fermions (MFs), respectively, in the superconducting state.

By carefully examining the low-energy effective Hamiltonian, we also reveal that doped Dirac semimetals favor an equal-spin odd-parity pairing rather than a conventional s -wave one. The former pairing exhibits a distinct quartet of surface MFs stemming from the FL, though point nodes exist when the system retains C_4 rotation symmetry. If the C_4 symmetry is reduced to C_2 by a structural phase transition, the nodes disappear, and a full-gapped symmetry-protected TSC is realized. The FL-induced MFs are clearly distinguished from those in other TSCs [47, 48] including superfluid $^3\text{He-A}$ [49, 50] and Weyl superconductors [33, 51–54]. We finally suggest possible application of our theory to recently discovered superconducting states in Cd_3As_2 and Au_2Pb .

Stability of Dirac points and surface Fermi loop—First, we provide a general argument on the topology of Dirac points. Our theory assumes TRS, IS, and uniaxial rotation symmetry, which are the most common symmetries for Dirac semimetals. In the presence of TRS and IS, Kramer’s degeneracy exists at arbitrary \mathbf{k} in the BZ, ensuring fourfold degeneracy when the conduction and valence bands are in contact. Such an accidental band crossing is generally not stable owing to band repulsion. However, if the band-touching point is on the high-symmetry axis, a C_n symmetry can retain the band crossing as a Dirac point [1–4]. Below we clarify the relevant topological structures.

We focus on the C_4 symmetric Hamiltonian, $C_4 H(\mathbf{k}) C_4^{-1} = H(R_4 \mathbf{k})$, with $R_4 \mathbf{k} = (k_y, -k_x, k_z)$. Here, without losing generality, we have chosen the rotation axis as the k_z axis. The commutation relations between

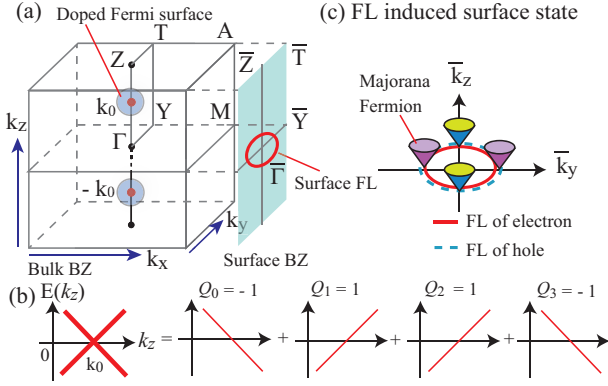


FIG. 1. (Color online) (a) Schematic picture of the Dirac points at $(0, 0, \pm k_0)$ and the surface Fermi FL in the bulk BZ and the surface BZ, respectively. (b) On the k_z -axis, a bulk Dirac point with $Q = -1$ in the left-hand side is decomposed into four chiral modes with different α_p in the right-hand side. The bold line is doubly degenerate. (c) Schematic illustration of the surface Majorana quartet in the superconducting Dirac semimetal.

the TRS operator T , IS operator P , and C_4 are summarized as $[T, P] = [T, C_4] = [P, C_4] = 0$. As illustrated in Fig. 1(a), for a C_4 symmetric tetragonal crystal, there are two C_4 symmetry lines, $\Gamma Z = (0, 0, k_z)$ and $MA = (\pi, \pi, k_z)$, with $k_z \in [-\pi, \pi]$. On these C_4 symmetry lines, the Hamiltonian commutes with C_4 ; thus, any energy band along the high-symmetry lines has a definite eigenvalue of the C_4 operator, $\alpha_p = \exp\left[\frac{i\pi}{2}\left(p + \frac{1}{2}\right)\right]$ ($p = 0, 1, 2, 3$).

The existence of Dirac points is ensured by the topological invariant defined below. The system is generally gapped at the C_4 symmetry points $k = \Gamma, Z, M, A$, so one can count the number of bands below the Fermi level at these points. Denoting the number of such bands with the C_4 eigenvalue α_p at k as $N_p(k)$, we can introduce the topological number, $\mathcal{Q}_p = N_p(\Gamma) - N_p(Z)$, for Dirac points on the ΓZ line, which we call the C_4 topological invariant. The Kramer's degeneracy due to PT symmetry requires $\mathcal{Q}_p = \mathcal{Q}_{3-p}$ ($p = 0, 1$). Moreover, the sum rule $\sum_{p=0}^3 \mathcal{Q}_p = 0$ holds for Dirac semimetals. Indeed, for a Dirac semimetal to become an insulator by a small C_4 breaking perturbation, the total number of bands below the Fermi level should be the same at all the symmetry points k , which leads to the sum rule. From these two relations, we have

$$\mathcal{Q}_0 = -\mathcal{Q}_1 = -\mathcal{Q}_2 = \mathcal{Q}_3 \equiv \mathcal{Q}. \quad (1)$$

If $\mathcal{Q} \neq 0$, any band with α_p has \mathcal{Q} gapless points on the ΓZ lines, corresponding to the difference $N_p(\Gamma) - N_p(Z)$, which eventually form \mathcal{Q} Dirac points. In Fig. 1(b), we illustrate a Dirac point with $Q = -1$. Because band mixing between different C_4 eigensectors is prohibited, the resultant Dirac points are stable as long as C_4 symmetry is maintained. Similarly, we can also introduce the C_4

invariant for Dirac points on the MA line.

Because of IS and the C_2 subgroup for C_4 symmetry, the system also has mirror reflection symmetry, $M_{xy}H(k_x, k_y, k_z)M_{xy}^{-1} = H(k_x, k_y, -k_z)$, with $M_{xy} = C_4^2P$. In the mirror-invariant planes ($k_z = 0$ or π), the Hamiltonian is block-diagonal in the basis of the eigenstates of M_{xy} ; thus, the mirror Chern number $\nu_\lambda(k_z)$ with $k_z = 0, \pi$ is defined as $\nu_\lambda(k_z) := 1/2\pi \int_{\text{BZ}} dk_x dk_y \mathcal{F}^\lambda(\mathbf{k})$, with $\mathcal{A}_a^\lambda(\mathbf{k}) := \sum_{E_n < 0} i \langle u_n^\lambda(\mathbf{k}) | \partial_{k_a} u_n^\lambda(\mathbf{k}) \rangle$ [55, 56], where $|u_n^\lambda(\mathbf{k})\rangle$ is an eigenstate of $H(\mathbf{k})$ in the mirror sector with the eigenvalue $\lambda = \pm i$ of M_{xy} and \mathcal{F}^λ is the field strength of \mathcal{A}_a^λ . Generalizing the relation between a band inversion and the Chern number in terms of eigenvalues of crystal symmetry [42, 57–60], we obtain the following relation for the mirror Chern number:

$$e^{\frac{i\pi}{2}\nu_\lambda(0)} = \prod_p \alpha_p^{[N_{(p,\lambda)}(\Gamma) + N_{(p,\lambda)}(M)]} \prod_q \xi_q^{-\mathcal{N}_{(q,\lambda)}(Y)}, \quad (2)$$

where $\xi_q = \exp\left[i\pi\left(q + \frac{1}{2}\right)\right]$ ($q = 0, 1$) is the eigenvalue of C_2 , $N_{(p,\lambda)}(k)$ is the number of occupied bands at k with a set of the C_4 and M_{xy} eigenvalues (α_p, λ) , and $\mathcal{N}_{(q,\lambda)}(Y)$ are those at Y with a set of C_2 and M_{xy} eigenvalues (ξ_q, λ) . [Y is the C_2 symmetry point in Fig. 1(a)]. Note that occupied bands at the C_4 (C_2) symmetry points have a definite set of eigenvalues for C_4 (C_2) and M_{xy} because $[C_4, M_{xy}] = [C_2, M_{xy}] = 0$. We can also obtain a similar relation for $\nu_\lambda(\pi)$ by replacing Γ, M , and Y with Z, A , and T , respectively, in Fig. 1(a).

To see the close relationship between the C_4 invariant and the mirror Chern number, consider a process in which a pair of stable Dirac points is created at Γ [4]. Band inversion at Γ occurs in this process, so a Kramer's pair of occupied bands, which have a set of eigenvalues $(\alpha_{p'}, \lambda)$ and $(\alpha_{3-p'}, -\lambda) \equiv (\alpha_{p'}^*, \lambda^*)$, go above the Fermi level, and a Kramer's pair of empty bands with the eigenvalues $(\alpha_{p''}, \lambda)$ and $(\alpha_{3-p''}, -\lambda)$ go below it at Γ . As a result, $N_{(p,\lambda)}(\Gamma)$ changes by $\Delta N_{(p',\lambda)}(\Gamma) = \Delta N_{(3-p',-\lambda)}(\Gamma) = -1$, $\Delta N_{(p'',\lambda)}(\Gamma) = \Delta N_{(3-p'',-\lambda)}(\Gamma) = 1$. To have a stable Dirac point, \mathcal{Q}_p should change at the same time, so $p' \neq p''$. Then, from Eq. (2), we find that this process induces a simultaneous change in the mirror Chern number $\Delta\nu_\lambda(0)$:

$$\begin{aligned} \Delta\nu_\lambda(0) &= \sum_p \left(p + \frac{1}{2}\right) \Delta N_{(p,\lambda)}(\Gamma) \pmod{4}, \\ &= (p'' - p') \neq 0 \pmod{4}. \end{aligned} \quad (3)$$

Therefore, the creation of stable Dirac points is always accompanied by a net change in the mirror Chern number. From the bulk-boundary correspondence, the resultant mirror Chern number ensures the existence of surface helical Dirac fermions, whose Fermi surfaces form FLs.

Although the surface FL accompanies bulk Dirac points, it can be stable even when C_4 symmetry is lost,

so the Dirac points have gaps. Indeed, unless the C_2 subgroup is broken, the system maintains mirror reflection symmetry, which is sufficient to stabilize the surface FL. Therefore, the structural phase transition that breaks C_4 to C_2 retains the FL.

Topology of superconducting Dirac semimetals— With a finite carrier density, Dirac semimetals have disconnected bulk Fermi surfaces, each of which surrounds one of the band-touching Dirac points. See Fig. 1(a). Now consider a superconducting state in Dirac semimetals. The system is described by the Bogoliubov–de Gennes (BdG) Hamiltonian,

$$H_{\text{BdG}}(\mathbf{k}) = \begin{pmatrix} H(\mathbf{k}) - \mu & \Delta(\mathbf{k}) \\ \Delta^\dagger(\mathbf{k}) & -H^*(-\mathbf{k}) + \mu \end{pmatrix}, \quad (4)$$

where $H(\mathbf{k})$ is the Hamiltonian for Dirac semimetals discussed above, μ is the chemical potential corresponding to the finite carrier density, and $\Delta(\mathbf{k})$ is the gap function. The BdG Hamiltonian supports particle–hole symmetry, $CH_{\text{BdG}}(\mathbf{k})C^{-1} = -H_{\text{BdG}}(-\mathbf{k})$, $C = \tau_x K$, with the Pauli matrix τ_x in the Nambu space and the conjugation operator K . Moreover, it may retain the symmetries of Dirac semimetals, depending on the symmetry property of the gap function. In particular, for a gap function with $C_4\Delta(\mathbf{k})C_4^\dagger = e^{-\frac{i\pi r}{2}}\Delta(R_4\mathbf{k})$ ($r = 0, \dots, 3$), $H_{\text{BdG}}(\mathbf{k})$ keeps C_4 symmetry, $\tilde{C}_4 H_{\text{BdG}}(\mathbf{k}) \tilde{C}_4^{-1} = H_{\text{BdG}}(R_4\mathbf{k})$, with $\tilde{C}_4 = \text{diag}[C_4, e^{\frac{i\pi r}{2}} C_4^*]$. In addition, for a mirror-even or mirror-odd gap function that satisfies $M_{xy}\Delta(\mathbf{k})M_{xy}^\dagger = \eta_M\Delta(k_x, k_y, -k_z)$ with $\eta_M = \pm 1$, the system retains mirror reflection symmetry, $\tilde{M}_{xy}H_{\text{BdG}}(\mathbf{k})\tilde{M}_{xy}^{-1} = H_{\text{BdG}}(k_x, k_y, -k_z)$, with $\tilde{M}_{xy} = \text{diag}[M_{xy}, \eta_M M_{xy}^*]$. Correspondingly, we can introduce the C_4 -invariant \tilde{Q}_p and the mirror Chern numbers $\tilde{\nu}_\lambda$ for $H_{\text{BdG}}(\mathbf{k})$ [40, 41], in a manner similar to that used for those of $H(\mathbf{k})$. The topological numbers \tilde{Q}_p and $\tilde{\nu}_\lambda$ are responsible for the existence of bulk point nodes on the ΓZ line and surface MFs in the superconducting state, respectively.

To evaluate these topological numbers, we employ the weak pairing assumption [30, 31, 34], i.e., that the superconducting gap is much smaller than the Fermi energy. The gap function is reasonably negligible away from the Fermi surface, in which we can take $\Delta(\mathbf{k}) \rightarrow 0$, leading to $H_{\text{BdG}}(\mathbf{k}) \rightarrow \text{diag}[H(\mathbf{k}) - \mu, -H^*(-\mathbf{k}) + \mu]$. Therefore, at the symmetry points $k = \Gamma, Z, M, A$, we can relate the negative energy states of $H_{\text{BdG}}(k)$ to those of $H(k)$. By taking into account the contribution from holes as well as electrons, the number \tilde{N}_p of negative energy states with the \tilde{C}_4 eigenvalue α_p is evaluated as $\tilde{N}_p(k) = N_p(k) + [N - N_{p_h}(k)]$, where N is the total number of bands in $H(\mathbf{k})$, $p_h = 3 - p + r \pmod 4$, and the first (second) term on the right-hand side comes from the electron (hole) contribution. From this equation, the C_4

invariant in the superconducting state is obtained as

$$\tilde{Q}_p = \begin{cases} 0 & r = 0 \text{ or } p = p_h, \\ 2Q_p & \text{otherwise.} \end{cases} \quad (5)$$

Similarly, the mirror Chern number in the superconducting state is calculated as the sum of the electron and hole mirror Chern numbers, $\tilde{\nu}_\lambda = \nu_\lambda + \nu_{\lambda_h}$, with $\lambda_h = -\eta_M\lambda$. As TRS in Dirac semimetals implies $\nu_{-\lambda} = -\nu_\lambda$, we have

$$\tilde{\nu}_\lambda = \begin{cases} 0 & \eta_M = 1, \\ 2\nu_\lambda & \eta_M = -1. \end{cases} \quad (6)$$

Relations (5) and (6) have important physical consequences. (i) In the presence of C_4 symmetry, any superconducting Dirac semimetal with a nontrivial r ($r = 1, 2, 3$) hosts point nodes as a remnant of Dirac points. Indeed, Eqs. (1) and (5) imply that at least a couple of \tilde{Q}_p are nonzero in this case. To open a point node gap, we need to break the C_4 rotation symmetry. (ii) If the gap function is mirror-odd, the mirror Chern number of the superconducting Dirac semimetal is nonzero, resulting in double MFs. In Fig. 1(c), we illustrate how the double MFs are created. In general, the gap function mixes the surface FL of electrons with that of holes so as to open a gap for the FL. In the mirror-odd case, however, mixing is prohibited on the mirror-invariant line in the surface BZ, so a pair of gapless points remains for each FL, forming double MFs.

In addition to the double MFs on the mirror-invariant line, we also find that each FL in the mirror-odd superconductor creates another pair of MFs *on the k_z axis in the surface BZ*. By combining with C and \tilde{M}_{xy} , the BdG Hamiltonian for the surface FL on the k_z axis, which we denote $H_{\text{BdG}}^{\text{FL}}(k_z)$, has antiunitary antisymmetry, $C_M H_{\text{BdG}}(k_z) C_M^{-1} = -H_{\text{BdG}}^{\text{FL}}(k_z)$, with $C_M = i\tilde{M}_{xy}C = i\tilde{M}_{xy}\tau_x K$. Because $C_M^2 = 1$ in the mirror-odd superconductor, $H_{\text{BdG}}^{\text{FL}}(k_z) i\tilde{M}_{xy}\tau_x$ is found to be real antisymmetric; thus, by using the Pfaffian, we can introduce the zero-dimensional topological invariant $\chi(k_z) = \text{sgn}\{\text{Pf}[H_{\text{BdG}}^{\text{FL}}(k_z) i\tilde{M}_{xy}\tau_x]\}$. In the weak pairing case, $\chi(k_z)$ is evaluated as $\chi(k_z) = \text{sgn}\{\det[H^{\text{FL}}(k_z) - \mu]\}$, where $H^{\text{FL}}(k_z) - \mu$ is the Hamiltonian of the surface FL on the k_z axis [61]. Therefore, $\chi(k_z)$ has different signs inside and outside the FL, which implies that $H_{\text{BdG}}^{\text{FL}}(k_z)$ should have zero-energy states near the points of intersection between the FL and the k_z axis. These zero-energy states form a pair of MFs on the k_z axis. Consequently, we can conclude that each FL has a quartet of MFs, as shown in Fig. 1(c). The quartet of MFs can stay gapless even when C_4 symmetry is broken, as long as mirror symmetry is preserved.

Low-energy analysis and application to Cd_3As_2 .— For definiteness, we study the low-energy effective Hamiltonian, which describes a class of Dirac semimetals including Cd_3As_2 and Au_2Pb . Because bands in Dirac

semimetals are doubly degenerate owing to PT symmetry, band-touching Dirac points are minimally described by a 4×4 matrix Hamiltonian. Thus, in the minimal setup, we need orbital degrees of freedom in addition to spin degrees of freedom, which are given by the Pauli matrices σ_μ and s_μ in the orbital (1, 2) and spin (\uparrow, \downarrow) spaces, respectively. The form of the 4×4 Hamiltonian is uniquely determined by symmetry [3, 4]. In particular, for $P = \pm\sigma_z$, the low-energy lattice Hamiltonian is given by [4]

$$\begin{aligned} H(\mathbf{k}) = & \{M - t_{xy}(\cos k_x + \cos k_y) - t_z \cos k_z\} \sigma_z s_0 \\ & + (\eta \sin k_x) \sigma_x s_z - (\eta \sin k_y) \sigma_y s_0 \\ & + (\beta + \gamma) \sin k_z (\cos k_y - \cos k_x) \sigma_x s_x \\ & - (\beta - \gamma) (\sin k_z \sin k_x \sin k_y) \sigma_x s_y, \end{aligned} \quad (7)$$

with $T = i\sigma_0 s_y K$ and $C_4 = e^{i\frac{\pi}{4}(2+\sigma_z)s_z}$. Here M , t_{xy} , t_z , η , β , and γ are material-dependent real constants. If $t_z > (M - 2t_{xy}) > 0$, this model has a pair of Dirac points located at $\mathbf{k} = (0, 0, \pm k_0)$, with $k_0 > 0$ defined by $M = t_z \cos k_0 + 2t_{xy}$. We find $\nu_{\pm i}(0) = \pm 1$ and $|\mathcal{Q}| = 1$. Accordingly, the FL arises at the surface parallel to the k_z axis, and the Dirac points are protected by C_4 .

Near the Dirac points at $\mathbf{k} = (0, 0, \pm k_0)$, the low-energy Hamiltonian takes the form of the Dirac Hamiltonian, $H(\mathbf{k}) = \pm t_z k_0 (k_z \mp k_0) \sigma_z s_0 + \eta(k_x \sigma_x s_z - k_y \sigma_y s_0)$, which exhibits nontrivial *orbit-momentum locking*. In Fig. 2(a), we show orbital textures in the $k_x k_y$ plane with $k_z = \pm k_0$ in each spin sector, where the orientation of the orbit is tightly locked to the direction of the momentum on the Fermi surface. Orbit-momentum locking critically affects the possible pairing symmetry in the superconducting state. Indeed, we can show that constant s -wave pairing is inconsistent with the orbital texture. First, in such a static pairing state, electrons forming the Cooper pair have opposite momentum to each other, so they must belong to different Dirac points. Furthermore, as an s -wave pairing is spin-singlet, it must be formed between electrons in different spin sectors. However, for a Cooper pair between electrons in different Dirac points and different spin sectors, orbit-momentum locking requires a momentum-dependent orbital structure in the Cooper pairing, as illustrated in Fig. 2(a). Therefore, even if the pairing interaction favors an s -wave superconducting state, the pairing function cannot be constant, suggesting suppression of the critical temperature.

On the other hand, for a Cooper pair with parallel spins, orbit-momentum locking is consistent with a constant pairing function. Indeed, the orbital-singlet equal-spin pairing, $\Delta = \Delta_0(c_{\uparrow,1}c_{\uparrow,2} - c_{\downarrow,2}c_{\downarrow,1}) + i\Delta'_0(c_{\uparrow,1}c_{\uparrow,2} + c_{\downarrow,2}c_{\downarrow,1})$ ($\equiv \Delta_{\parallel}$) is compatible with the orbital texture in Fig. 2(a). Such an orbital-singlet Cooper pair is realized when the effective pairing interaction is dominated by an attractive interorbital interaction $\mathcal{H}_{\text{int}} = -2Vn_1n_2$, with $n_\sigma = \sum_{s=\uparrow,\downarrow} c_{s,\sigma}^\dagger(\mathbf{x})c_{s,\sigma}(\mathbf{x})$ ($V > 0$) [30, 62–64]. Although the actual pairing interaction is

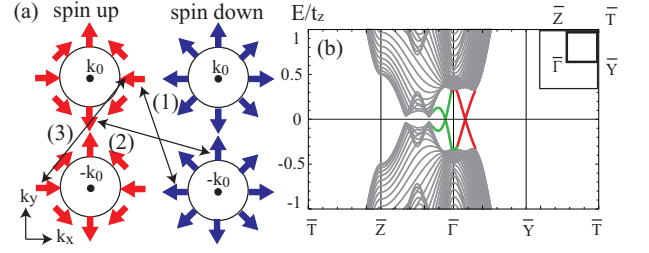


FIG. 2. (Color online) (a) Orbital textures on the Fermi surfaces in the $k_x k_y$ -plane with $k_z = \pm k_0$ in the $s_z = 1$ (left) and $s_z = -1$ (right) sectors. Arrows indicate the direction of the orbit, $(\langle \sigma_x \rangle, \langle \sigma_y \rangle)$. A Cooper pair between electrons with opposite spin may realize both of a parallel orbit pair (1) and an anti-parallel one (2), depending on the momentum. On the other hand, a Cooper pair between electrons in the same spin state always have the anti-parallel orbit configuration (3). (b) Energy spectra at the (100) face. $\mu/t_z = 0.5$, $M/t_z = 4$, $t_{xy}/t_z = 2$, $\eta/t_z = 1$, $\beta/t_z = 2$, $\gamma/t_z = 1$, $\Delta_0/t_z = 0.1$, $\Delta'_0/t_z = 0.01$, and $m_0/t_z = 0.2$. The distance between left ($x = 0$) and right ($x = L$) surfaces is $L = 50$. The red and green lines show the FL induced MFs.

material-dependent, the above results imply that doped Dirac semimetals favor the latter gap function. Because Δ_{\parallel} is C_4 -symmetric with $r = 2$ and mirror-odd, i.e., $C_4 \Delta_{\parallel} C_4^\dagger = -\Delta_{\parallel}$, it realizes a symmetry-protected TSC with bulk point nodes and a surface MF quartet, as discussed previously. In Fig. 2(b), we illustrate the quartet of MFs in this phase by numerically calculating the surface energy spectrum of the BdG Hamiltonian with Eq. (7) and $\Delta = \Delta_{\parallel}$. Here we have also taken into account a symmetry-lowering effect from C_4 to C_2 by phenomenologically adding $(m_0 \sin k_z) \sigma_x s_x$ to Eq. (7). As expected, Fig. 2(b) proves the existence of MFs on the mirror-invariant line ($\bar{\Gamma}\bar{Y}$) and the k_z axis ($\bar{\Gamma}\bar{Z}$) and moreover shows a gap in the $\bar{Z}\bar{\Gamma}$ direction due to the C_4 breaking term [65]. The obtained MFs in the mirror-invariant plane stay gapless even if the interaction effects are taken into account [67, 68].

Finally, we discuss possible application of our theory to superconductivity in Au_2Pb and Cd_3As_2 . For Au_2Pb , first-principle calculations show that the Fermi level of this material is inside the gap of the Dirac points [26]; thus, no electron near the Dirac points contributes to the Cooper pairs. Hence, no TSC as discussed above is expected in Au_2Pb . On the other hand, the analysis above is applicable to the recently discovered superconductor Cd_3As_2 . In Cd_3As_2 , under high pressure, the structural phase transition occurs before the superconducting transition. Together with the orbit-momentum locking discussed above, the symmetry-lowering effect may stabilize the TSC phase by increasing the condensation energy, as the point nodes in the TSC phase are gapped when C_4 is reduced to C_2 . Therefore, it is likely that Cd_3As_2 realizes the TSC phase. The mirror-odd gap function of the TSC is detectable via anomalous Josephson ef-

fects [30, 66] with carefully fabricated junctions.

The authors are grateful to Y. Yanase for discussions. This work is supported in part by a Grant-in Aid for Scientific Research from MEXT of Japan, “Topological Quantum Phenomena,” Grant No. 22103005 and “Topological Material Science” (No. 15H05855) KAKENHI on innovation areas from MEXT. S.K. acknowledges support from JSPS (Grant No. 256466). M.S. is supported by Grant-Aid for scientific Research B (Grant No. 25287085) from JSPS.

-
- [1] S. M. Young, S. Zaheer, J. C. Y. Teo, C. L. Kane, E. J. Mele, and A. M. Rappe, *Phys. Rev. Lett.* **108**, 140405 (2012).
- [2] Z. Wang, Y. Sun, X.-Q. Chen, C. Franchini, G. Xu, H. Weng, X. Dai, and Z. Fang, *Phys. Rev. B*, **85**, 195320 (2012).
- [3] Z. Wang, H. Weng, Q. Wu, X. Dai, and Z. Fang, *Phys. Rev. B*, **88**, 125427 (2013).
- [4] B.-J. Yang and N. Nagaosa, *Nat. Commun.* **5**, 4898 (2014).
- [5] H. Yi, *et al.* *Sci. Rep.* **4**, 6106 (2014).
- [6] M. Neupane, *et al.*, arXiv:1501.00697v1 (2015).
- [7] X. Wan, A. M. Turner, A. Vishwanath, and S. Y. Savrasov, *Phys. Rev. B* **83**, 205101 (2011).
- [8] Z. K. Liu, *et al.*, *Science* **343**, 864 (2014).
- [9] S. Y. Xu, *et al.*, arXiv:1312.7824 (2013).
- [10] S. Y. Xu, *et al.*, *Science* **347**, 294 (2015).
- [11] S. K. Kushwaha, *et al.*, *APL Mat.* **3**, 041504 (2015).
- [12] M. Neupane, *et al.*, *Nat. Commun.* **5**, 3786 (2014).
- [13] S. Borisenko, Q. Gibson, D. Evtushinsky, V. Zabolotnyy, B. Büchner, and R. J. Cava, *Phys. Rev. Lett.* **113**, 027603 (2014).
- [14] Z. K. Liu, *et al.* *Nature Mater.* **13**, 677 (2014).
- [15] S. Jeon, *et al.* *Nature Mater.* **13**, 851 (2014).
- [16] L. P. He, X. C. Hong, J. K. Dong, J. Pan, Z. Zhang, J. Zhang, and S. Y. Li, *Phys. Rev. Lett.* **113**, 246402 (2014).
- [17] T. Liang, Q. Gibson, M. N. Ali, M. Liu, R. J. Cava, and P. N. Ong, *Nat. Mater.* **14**, 280 (2015).
- [18] Q. D. Gibson, *et al.*, *Phys. Rev. B* **91** 205128 (2015)
- [19] Y. Du, B. Wan, D. Wang, L. Sheng, C.-G. Duan, and X. Wan, arXiv:1411.4394v3 (2014).
- [20] J. A. Steinberg, S. M. Young, S. Zaheer, C. L. Kane, E. J. Mele, and A. M. Rappe, *Phys. Rev. Lett.* **112**, 036403 (2014).
- [21] A. Narayan, D. DiSante, S. Picozzi, and S. Sanvito, *Phys. Rev. Lett.* **113**, 256403 (2014).
- [22] E. M. Seibel, *et al.*, *J. Am. Chem. Soc.* **137**, 1282 (2015).
- [23] L. Aggarwal, *et al.*, arXiv:1410.2072 (2014).
- [24] H. Wang, *et al.*, arXiv:1501.00418 (2015).
- [25] L. P. He, *et al.*, arXiv:1502.02509 (2015).
- [26] L. M. Schoop, *et al.* *Phys. Rev. B* **91**, 214517 (2015).
- [27] S. Zhang, *et al.*, *Phys. Rev. B* **91**, 165133 (2015).
- [28] M. Sato, *Phys. Lett. B* **575**, 126 (2003).
- [29] L. Fu and C. L. Kane, *Phys. Rev. Lett.* **100**, 096407 (2008).
- [30] L. Fu and E. Berg, *Phys. Rev. Lett.* **105**, 097001 (2010).
- [31] X.-L. Qi, T. L. Hughes, and S.-C. Zhang, *Phys. Rev. B* **81**, 134508 (2010).
- [32] A. Yamakage, K. Yada, M. Sato, and Y. Tanaka, *Phys. Rev. B*, **85**, 180509(R) (2012).
- [33] B. Lu, K. Yada, M. Sato, and Y. Tanaka, *Phys. Rev. Lett.* **114**, 096804 (2015).
- [34] M. Sato, *Phys. Rev. B* **81**, 220504(R) (2010).
- [35] L. Fu, *Phys. Rev. Lett.* **106**, 106802 (2011).
- [36] C.-K. Chiu, H. Yao, and S. Ryu, *Phys. Rev. B* **88**, 075142 (2013).
- [37] T. Morimoto and A. Furusaki, *Phys. Rev. B* **88**, 125129 (2013).
- [38] K. Shiozaki and M. Sato, *Phys. Rev. B* **90**, 165114 (2014).
- [39] S. Kobayashi, K. Shiozaki, Y. Tanaka, and M. Sato, *Phys. Rev. B*, **90**, 024516 (2014).
- [40] Y. Ueno, A. Yamakage, Y. Tanaka, and M. Sato, *Phys. Rev. Lett.* **111**, 087002 (2013).
- [41] F. Zhang, C L. Kane, and E. J. Mele, *Phys. Rev. Lett.* **111**, 056403 (2013).
- [42] C. Fang, M. J. Gilbert, X. Dai, and B. A. Bernevig, *Phys. Rev. Lett.* **108**, 266802 (2012).
- [43] A. Alexandradinata, C. Fang, M. J. Gilbert, and B. A. Bernevig, *Phys. Rev. Lett.* **113**, 116403 (2014).
- [44] R.-J. Slager, A. Mesaros, V. Juricic, and J. Zaanen, *Nat. Phys.* **9**, 98 (2013).
- [45] S. A. Yang, H. Pan, and F. Zhang, *Phys. Rev. Lett.* **113**, 046401 (2014).
- [46] M. Koshino, T. Morimoto, and M. Sato, *Phys. Rev. B*, **90**, 115207 (2014).
- [47] Y. Tanaka, M. Sato, and N. Nagaosa, *J. Phys. Soc. Jpn.* **81**, 0111013 (2012).
- [48] X. L. Qi and S. C. Zhang, *Rev. Mod. Phys.* **83**, 1057 (2011).
- [49] N. B. Kopnin and M. M. Salomaa, *Phys. Rev. B* **44**, 9667 (1991).
- [50] G. E. Volovik, *Lect. Notes in Phys.* **870** (2013).
- [51] T. Meng and L. Balents, *Phys. Rev. B* **86**, 054504 (2012).
- [52] G. Y. Cho, J. H. Bardarson, Y.-M. Lu, and J. E. Moore, *Phys. Rev. B* **86**, 214514 (2012).
- [53] P. Hosur, X. Dai, Z. Fang, and X.-L. Qi, *Phys. Rev. B*, **90**, 045130 (2014).
- [54] V. Shivamoggi and M. J. Gilbert, *Phys. Rev. B* **88**, 134504 (2013).
- [55] J. C. Y. Teo, L. Fu, and C. L. Kane, *Phys. Rev. B* **78**, 045426 (2008).
- [56] T. Heish, H. Liu, J. Liu, W. Duan, A. Bansil, and F. Fu, *Nat. Commun.* **3**, 982 (2012).
- [57] L. Fu and C. L. Kane, *Phys. Rev. B* **76**, 045302 (2007).
- [58] M. Sato, *Phys. Rev. B* **79**, 214526 (2009).
- [59] C. Fang, M. J. Gilbert, and B. A. Bernevig, *Phys. Rev. B* **86**, 115112 (2012).
- [60] W. A. Benalcazar, J. C. Y. Teo, and T. L. Hughes, *Phys. Rev. B*, **89**, 224503 (2014).
- [61] See the Supplemental Material at [URL will be inserted by publisher] for the detail calculation.
- [62] S. Nakosai, Y. Tanaka, and N. Nagaosa, *Phys. Rev. Lett.* **108**, 147003 (2012).
- [63] T. Mizushima, A. Yamakage, M. Sato, and Y. Tanaka, *Phys. Rev. B* **90**, 184516 (2014).
- [64] P. M. R. Brydon, S. Das Sarma, H.-Y. Hui, and J. D. Sau, *Phys. Rev. B* **90**, 184512 (2014).
- [65] The obtained TSC cannot be considered as a stack of lower dimensional topological phases. In this sense, it is a strong phase.
- [66] A. Yamakage, M. Sato, K. Yada, S. Kashiwaya, and

- Y. Tanaka, Phys. Rev. B **87**, 100510(R) (2013).
[67] Z.-C. Gu and M. Levin, Phys. Rev. B **89**, 201113(R) (2014).
[68] Y. Qi and L. Fu, arXiv:1505.06201v1 (2015).